

# A dynamic mathematical model for once-through boiler-turbine units with superheated steam temperature<sup>☆</sup>

He Fan<sup>a</sup>, Zhi-gang Su<sup>a,\*</sup>, Pei-hong Wang<sup>a,\*</sup>, Kwang Y. Lee<sup>b</sup>

<sup>a</sup> School of Energy and Environment, Southeast University, Nanjing, Jiangsu 210096, China

<sup>b</sup> Department of Electrical and Computer Engineering, Baylor University, Waco, TX 76706, USA



## HIGHLIGHTS

- Influence of spray water is considered in modeling coordinated control system.
- Effect of total feedwater flow is analyzed in modeling temperature system.
- Correction factors of heat function are modeled to improve model accuracy.
- Model structure shows the varying inertia and nonlinearity of temperature system.
- The model is validated by both systems of a 1000 MW once-through boiler unit.

## ARTICLE INFO

### Keywords:

Once-through boiler-turbine  
Dynamic mathematical model  
Superheated steam temperature  
Coordinated control system  
Controller design

## ABSTRACT

To absorb more renewable energy generation into power grid, once-through boiler-turbine (OTBT) units are now required to operate in a wide load range while maintaining high safety and efficiency. Superheated steam temperature (SST), adjusted by spray water and feedwater together, plays a critical role on operational safety and economy. However, the models of OTBT units in existing literature have not reflected this essential inter-relationship, which may deteriorate the control performances of coordinated control system (CCS) and SST system. To this end, this study proposes to develop such a dynamic mathematical model of OTBT units. Model structure is derived from mass and energy conservation laws, and static parameters and functions are identified based on running data by using nonlinear regression analysis and optimization algorithm. Dynamic validation and open-loop simulation illustrate that the model has satisfactory accuracy, reflecting essential characteristics, and thus it can be used for simulation analysis and controller design.

## 1. Introduction

In recent years, renewable energy has been increased dramatically and made considerable economic and environmental contributions in China due to clean merits [1–3]. However, the intermittent and random nature of renewable energy (e.g. wind and solar energy) poses a threat to stable and safe operation of power grid, which results in a serious problem that a significant amount of renewable energy generation is wasted [1]. To resolve this problem, an effective solution is that operational flexibility of coal-fired units is improved to absorb renewable energy generation into power grid [4]. Here, operational flexibility involves load change rate, load change range and load regulation accuracy. By the end of 2016, installed capacity of over 300,000 kW coal-fired units accounted for 88.3% in China, and 600,000 kW and 1 million

kW-class units accounted for 46.7% [5]. Therefore, once-through boiler-turbine (OTBT) units are required to improve the operational flexibility and undertake environmental and social responsibilities, such as peak shaving, frequency regulation and ultra-low emissions of pollutants.

High operational flexibility of OTBT units depends on the coordinated control system (CCS) with good performance. However, frequent load change and varying coal quality can deteriorate control performance of superheated steam temperature (SST) and then threaten operational safety of OTBT units, which restricts the improvement of operational flexibility. Therefore, it is meaningful to research how to improve operational flexibility of OTBT units under the premise of safe operation.

Coordinated control system (CCS) and superheated steam temperature (SST) control system play an vital role in safe and economical

<sup>☆</sup> This research has been supported by National Nature Science Foundation of China (51676034).

\* Corresponding authors.

E-mail addresses: [zhigangsu@seu.edu.cn](mailto:zhigangsu@seu.edu.cn) (Z.-g. Su), [phwang@seu.edu.cn](mailto:phwang@seu.edu.cn) (P.-h. Wang).

Nomenclature		R <sup>2</sup>	Degree that dependent variables change with independent variables
$u_B$	Coal flow command (kg/s)	$E$	Error criterion
$r_B$	Pulverized-coal flow in furnace (kg/s)	$V$	Boiler volume (m <sup>3</sup> )
$r_{B1}$	Mass flow of raw coal in mill (kg/s)	Subscripts	
$r_{B2}$	Mass flow of pulverized-coal at output of mill (kg/s)	$m$	State in separator
$\tau$	Delay time of pulverized-coal system (s)	$fw$	Feed water
$\tau_1$	Coal transmission time in coal feeder (s)	$st$	State at throttle valve
$\tau_2$	Accumulation time in mill (s)	$r$	State in reheat
$\tau_3$	Delivery time in primary air pipe (s)	$r_1$	Reheated steam state at inlet of reheat
$M$	Amount of coal in the mill (kg)	$r_2$	Reheated steam state at outlet of reheat
$c_0$	Milling inertia time (s)	$sw1$	Primary spray water
$p$	Steam pressure (MPa)	$sw2$	Secondary spray water
$\rho$	Steam density (kg/m <sup>3</sup> )	5	State at output of low temperature superheat
$D$	Steam or water mass flow rate (kg/s)	4	State at input of platen superheat
$T$	temperature (°C)	3	State at output of platen superheat
$h$	Specific enthalpy (kJ/kg)	2	State at input of high temperature superheat
$k_{11}$	Energy absorbed by steam in economizer, waterwall and low temperature superheat by burning 1 kg coal (kJ/kg)	$sw$	Spray water
$k_{12}$	Energy absorbed by steam in platen superheat by burning 1 kg coal (kJ/kg)	Abbreviations	
$k_{13}$	Energy absorbed by steam in high temperature superheat by burning 1 kg coal (kJ/kg)	OTBT	Once-through boiler-turbine
$k_2$	Turbine coefficient	CCS	Coordinated system control
$\alpha$	Operating condition constant ( $0 \leq \alpha \leq 0.5$ )	SST	Superheated steam temperature
$\lambda$	Operating condition constant	RCW	Ratio of coal to water
$u_t$	Throttle valve opening ( $0 \leq u_t \leq 1$ )	MRE	Mean relative error
$N_e$	Unit load (MW)	RMSE	Root mean squared error
$\eta$	Turbine absolute internal efficiency (%)		

operation of power plants. As the core of control systems in power plants, CCS views boiler system with large delay and system inertia and turbine system with fast responses as a whole to track load command quickly while stabilizing main steam pressure. In addition, the SST is the highest steam temperature in a power plant, and thus it should be strictly controlled to be within a safe range in order to prevent a series of operating accidents, such as unplanned shutdown and tube crack [6,7]. Satisfactory control performance depends on accuracy and characteristics of process models, which have been made great progresses in these topics.

For models of CCS, the modeling methods can be roughly summarized in three types, namely, white-box modeling method, black-box modeling method and grey-box modeling method. White-box model is derived from mass, energy and momentum conservation laws, which can capture essential characteristics of physical processes. Parameters in the model can reflect its physical meaning and can be determined from design data [8,9]. Black-box model is the so-called data-driven models based on various regression technologies and artificial intelligence techniques [10–15], and it is established by combining training data and network structure. Black-box model has satisfactory accuracies, but its model structure is unreliable due to the lack of relevant mechanism analysis. Lastly, grey-box model is a combination of black-box and white-box models. The model is derived from conservation laws, and unclear parameters or functions in mechanism equations are obtained by combining operating data and optimization or regression algorithms [16–24]. This kind of model has physical structure and proper accuracies improved by operating data, and it is suitable for simulation analysis and controller design [25–27]. Besides, boiler and turbine systems can also be simulated by advanced softwares, such as GSE [28] and APROS [29], and the softwares can describe dynamic responses of real power plant accurately. However, models based on softwares are not suitable for controller design due to their complexity.

It is meaningful for CCS design to analyze and master essential

boiler-turbine dynamics. Different from drum boiler units, feedwater in OTBT units flows through boiler directly without water circulation in a separator at nominal operation of OTBT units, and disturbances can easily influence the operational safety of OTBT units due to less boiler metal and working fluid. In drum boiler units, fuel flow provides heat energy to generate steam flow, and feedwater flow is to maintain drum level at a rational range [30]. However, for OTBT units, coal flow burns in furnace to heat working fluid, and feedwater is to generate enough steam flow to maintain safe operation. When coal flow increases, steam enthalpy and pressure gradually increase due to more heat energy, and lastly unit load rises up to a new level [31]. When feedwater flow increases, steam enthalpy gradually decreases. However, steam pressure and unit load will rise due to squeezed effect, and then decline due to unchanged coal flow [16,17]. Lastly, when throttle valve opening enlarges, steam pressure decreases quickly, but steam enthalpy nearly keeps unchanged due to invariant ratio of coal to water (RCW). As the heat energy stored in boiler releases, unit load raises at once and gradually drops down after releasing the energy [32,5].

Due to its own merits, grey-box modeling method is widely adopted to model thermal systems. For OTBT units, these papers [16,17,32] are major contributions on modeling CCS. In [16], a lumped dynamic model is established, derived from conservation laws, and the model with a relatively simple model structure can capture the essential dynamic characteristics. More importantly, the model can be used for controller design [5,33]. Even though SST can be maintained at the set value by spray water in this study [16], it does not consider the relationship between feedwater and spray water for SST system. Similarly, the study [17] simplifies spray water to calculate main steam enthalpy, and it does not accord with practical operation. Besides, many groups of dynamic parameters and relevantly complex model structure are not conducive to controller design. In [32], a simplified dynamic OTBT model in low load is developed with acceptable accuracy. At the low load working condition, SST easily deviates from the set value, and it does not analyze the thermal process in superheater deeply to

calculate main steam enthalpy. For OTBT units, spray water changes feedwater flow entering into economizer and thus influencing the control quality of intermediate-point enthalpy, and this may cause waterwall overheating seriously. Spray water adjusts SST and main steam enthalpy promptly, and the main steam enthalpy has a close relationship with unit load. Thus, to accord with practical operation, spray water should be considered in modeling CCS to further improve its control performance.

For SST control system models, many modeling methods can describe physical processes of SST control system, such as recursive extended least squares [34], transfer functions [6,7], mechanism modeling method [35] and least squares support vector machines [36]. These methods can describe dynamic responses of SST against spray water disturbances effectively. In practice, control engineers widely accept the models in the form of transfer function under different operating conditions widely [37], and advanced algorithms are tested based on the model to improve control performance [6,7]. In recent years, these papers [24,35] report new advances on modeling SST system based on conservation laws, but there are still some aspects that need to study further. Firstly, above work focus on subcritical coal-fired units rather than the OTBT units, and there are many differences between two kinds of units in terms of SST system. Secondly, the studies [24,35] divide SST system into many components and analyze heat transfer process in tube wall and steam sides. Furthermore, equations of radiation and heat convection are adopted to describe every component of the SST system, and it is inevitable to increase the complexity of physical structure and computational time. Thirdly, for OTBT units, spray water has limited ability of adjusting SST in protecting waterwall, and intermediate-point enthalpy has a major influence on SST. When the ratio of spray water to total feedwater flow exceeds a set value, feedwater flow needs to change to stabilize the intermediate-point enthalpy in a rational range in order to maintain safe operation of units. Therefore, it is necessary and meaningful to establish a dynamic model of SST system for OTBT units by using conservation laws, where the model can capture essential dynamic characteristics with a relevantly simple physical structure. Importantly, the control performance of SST system can be improved by combining the model with advanced control algorithms, such as predictive control, fuzzy control and adaptive control.

In summary, intermediate-point enthalpy is controlled around a set value to realize coarse adjustment of SST, and spray water can achieve dynamic and prompt adjustment of SST. Although CCS has a close relationship with SST system for OTBT units, previous studies do not reflect the important interaction, which may deteriorate control performance of both systems.

To fill this gap, CCS and SST system should be viewed as a whole to establish a model and analyze their interaction, and a relevant researches based on mechanism analysis should be performed to improve control performances of both systems for a wide range of load operation. Based on its dynamic characteristics and simple physical structure, many control algorithms can be tested to enhance their control performance. Therefore, the purpose of this study is to develop such a dynamic control model of CCS and SST system for OTBT units, where CCS and SST system are regarded as a thermodynamic system to analyze its characteristics by using the grey box modeling method. Its physical structure is derived from mass and energy conservation laws, and a wide range of load running data are used to improve model accuracy. After identifying parameters and functions in the model, it can reflect the dynamic characteristics of both systems with a simple form and general physical structure, and it has acceptable accuracies and can be used for simulation analysis and controller design.

## 2. Description of OTBT coal-fired units

The OTBT coal-fired units mainly consist of 600 MW and 1000 MW OTBT coal-fired units, and the latter has higher efficiency due to high steam parameters. Thus, a 1000 MW ultra-supercritical (USC) OTBT coal-fired unit is investigated in this study. Its boiler is an ultra-supercritical sliding-pressure once-through boiler, and its turbine is an ultra-supercritical single reheat condensing steam turbine. A structure diagram of a 1000 MW USC OTBT coal-fired unit is given in Fig. 1, and the components and main parameters of the unit are shown in Tables 1 and 2, respectively.

## 3. Modeling of USC OTBT units

### 3.1. Modeling for pulverized-coal system

As shown in Fig. 1, raw coal is transferred from bunker to coal mill through coal feeder, and then it is ground into coal powder, which is delivered by primary air into furnace. Therefore, dynamic of pulverizing system contains time delay and system inertia. The time delay mainly consists of coal transmission time in coal feeder ( $\tau_1$ ), accumulation time in mill ( $\tau_2$ ) and delivery time in primary air pipe ( $\tau_3$ ). The coal flow in the coal mill and furnace, respectively, can be given by

$$r_{B1} = u_{B1} e^{-(\tau_1 + \tau_2)s}, \quad (1)$$

$$r_B = r_{B2} e^{-\tau_3 s}. \quad (2)$$

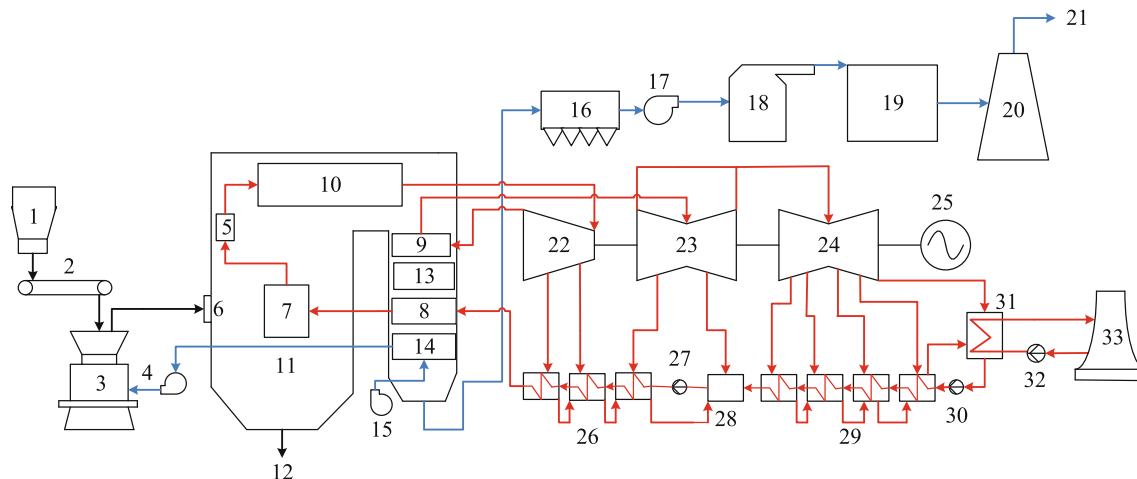


Fig. 1. Structure diagram of a 1000 MW USC coal-fired unit (black solid line: coal or coal powder flow; red solid line: steam or water flow; blue solid line: air or flue gas flow). (For interpretation of the references to colour in this figure legend, the reader is referred to the web version of this article.)

**Table 1**  
Components of a 1000 MW USC OTBT coal-fired unit.

Index	Component	Index	Component
1	Row coal bunker	18	Flue gas desulphur (FGD)
2	Coal feeder	19	Wet electrostatic precipitator (WESP)
3	Coal mill	20	Chimney
4	Primary fan	21	Flue gas
5	Separator	22	High-pressure (HP) turbine
6	Burner	23	Immediate-pressure (IP) turbine
7	Waterwall	24	Low-pressure (LP) turbine
8	Economizer	25	Generator
9	Reheater	26	HP feedwater heater
10	Superheater	27	Feedwater pump
11	Furnace	28	Degaerator
12	Coal cinder	29	LP feedwater heater
13	Selective catalytic reduction (SCR)	30	Condenser pump
14	Air preheater	31	Condenser
15	Force draft fan	32	Circulating water pump
16	Electrostatic precipitator (ESP)	33	Cooling tower
17	Induced draft fan		

**Table 2**  
Main parameters at Turbine Heat-Acceptance (THA) condition.

Item	Value
Rated power (MW)	1000
Superheated steam flow (t/h)	2732
Superheated steam pressure (MPa)	26.09
Superheated steam temperature (°C)	605
Reheated steam flow (t/h)	2276
Water temperature at inlet of economizer (°C)	291
Pressure at inlet of economizer (MPa)	29.65
Condenser pressure (kPa)	5.2

The inertia of pulverized-coal system mainly reflects mass change of coal in the mill, and the inertia is

$$\frac{dM}{dt} = r_{B2} - r_{B1} \quad (3)$$

Assuming that  $M = c_0 r_{B1}$  [17], and inserting (1) and (2) into (3) results in

$$c_0 \frac{dr_B}{dt} = -r_B + u_B e^{-(\tau_1 + \tau_2 + \tau_3)t}, \quad (4)$$

which can be further rewritten as

$$\frac{dr_B}{dt} = -\frac{1}{c_0} r_B + \frac{e^{-\tau t}}{c_0} u_B, \quad (5)$$

where  $\tau = \tau_1 + \tau_2 + \tau_3$ .

### 3.2. Modeling for boiler system

In boiler system, coal powder is fully burned in furnace to heat water and steam in tubes so as to generate superheated steam.

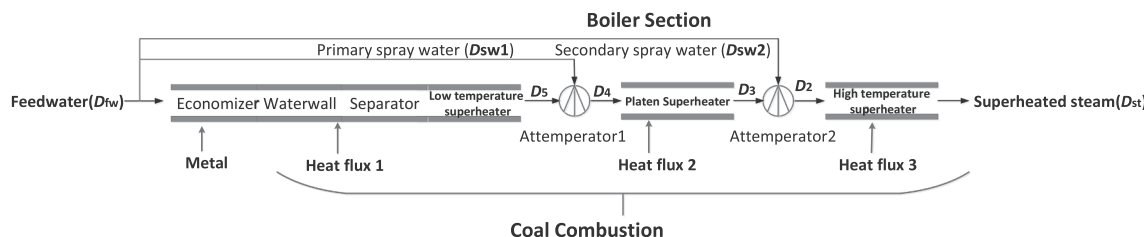


Fig. 2. A simplified structural diagram of once-through boiler section.

Considering the influence of spray water on CCS and SST system, this process can be simplified as shown in Fig. 2. Before modeling, some assumptions are presented as follows:

- (A1) Inertia of coal combustion and heat conduction is included in pulverized-coal system;
- (A2) As coal powder burns quickly in furnace, combustion time is ignored;
- (A3) Heat energy converted to working fluid in tube is nearly proportional to coal flow in furnace;
- (A4) Boiler is regarded as a whole tube with equal volume consisting of economizer, waterwall, separator and superheaters, as shown in Fig. 2;
- (A5) Heat energy released from coal combustion is distributed on the whole tube uniformly, and the varying rates of metal and steam temperatures are equal.

Based on aforementioned assumptions, a lumped parameter method is adopted in this study. Steam state in separator can reflect the change of ratio of coal to water (RCW) sensitively, and thus steam parameters in separator are chosen as lumped parameters. Steam enthalpy in separator can reflect the variation of RCW quickly and represent the energy of steam in separator. Therefore, enthalpy of steam in separator,  $h_m$ , is selected as an indicator that represents RCW in this study.

#### 3.2.1. Economizer, waterwall, separator and low temperature superheater

According to mass and energy conservation laws, we have

$$V_m \left( \frac{d\rho_m}{dt} \right) = D_{fw} - D_{sw1} - D_{sw2} - D_5, \quad (6)$$

$$\alpha_1 V_m \frac{d(\rho_m h_m)}{dt} = (D_{fw} - D_{sw1} - D_{sw2}) h_{fw} - D_5 h_5 + k_{11} r_B \quad (7)$$

with  $\alpha_1 = \alpha_1(x_1)$ , where  $V_m \left( \frac{d\rho_m}{dt} \right)$  and  $\alpha_1 V_m \frac{d(\rho_m h_m)}{dt}$  are mass change of working fluid in above components, kg/s, and energy change of working fluid and boiler metal in above components, kJ/s, respectively.

Combining (6) and (7), we can get derivatives of enthalpy and pressure of steam in separator as follows:

$$V_m \left( \frac{\partial \rho_m}{\partial p_m} \frac{dp_m}{dt} + \frac{\partial \rho_m}{\partial h_m} \frac{dh_m}{dt} \right) = D_{fw} - D_{sw1} - D_{sw2} - D_5, \quad (8)$$

$$\begin{aligned} \alpha_1 V_m \{ h_m \frac{\partial \rho_m}{\partial p_m} \frac{dp_m}{dt} + (h_m \frac{\partial \rho_m}{\partial h_m} + \rho_m) \frac{dh_m}{dt} \} \\ = (D_{fw} - D_{sw1} - D_{sw2}) h_{fw} - D_5 h_5 + k_{11} r_B, \end{aligned} \quad (9)$$

which can be simplified as

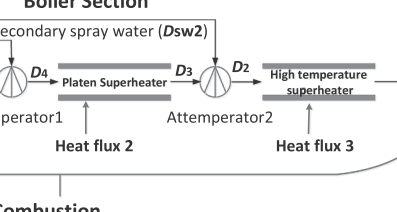
$$b_{11} \frac{dp_m}{dt} + b_{12} \frac{dh_m}{dt} = D_{fw} - D_{sw1} - D_{sw2} - D_5, \quad (10)$$

$$b_{21} \frac{dp_m}{dt} + b_{22} \frac{dh_m}{dt} = (D_{fw} - D_{sw1} - D_{sw2}) h_{fw} - l D_5 h_m + k_{11} r_B, \quad (11)$$

where

$b_{11} = V_m \frac{\partial \rho_m}{\partial p_m}$ ,  $b_{12} = V_m \frac{\partial \rho_m}{\partial h_m}$ ,  $b_{21} = \alpha_1 V_m h_m \frac{\partial \rho_m}{\partial p_m}$ ,  $b_{22} = \alpha_1 V_m (h_m \frac{\partial \rho_m}{\partial h_m} + \rho_m)$ , and  $l$  is the ratio of enthalpy of superheated steam at the output of low

#### Boiler Section



temperature superheater to that of steam in the separator(i.e.,  $l = \frac{h_5}{h_m}$ ).

With respect to  $\frac{dp_m}{dt}$  and  $\frac{dh_m}{dt}$ , (10) and (11) can be transformed to

$$c_{11}(\frac{dp_m}{dt}) = (h_{fw} - d_{11})(D_{fw} - D_{sw1} - D_{sw2}) + (d_{11} - lh_m)D_5 + k_{11}r_B, \quad (12)$$

$$c_{12}(\frac{dh_m}{dt}) = (h_{fw} - d_{12})(D_{fw} - D_{sw1} - D_{sw2}) + (d_{12} - lh_m)D_5 + k_{11}r_B \quad (13)$$

with  $c_{11} = b_{21} - \frac{b_{11}b_{22}}{b_{12}}$ ,  $c_{12} = b_{22} - \frac{b_{12}b_{21}}{b_{11}}$ ,  $d_{11} = \frac{b_{22}}{b_{12}}$  and  $d_{12} = \frac{b_{21}}{b_{11}}$ .

Differential pressure [16,17] of steam in boiler is

$$\Delta p = g_1(p_m), \quad (14)$$

where  $g_1(\cdot)$  is a nonlinear function, and  $\Delta p = p_m - p_s$  is steam pressure drop in low temperature superheater, MPa. As steam flow at output of low temperature superheater,  $D_5$ , can be measured in practical operation, we refer to main steam flow [38] and define  $D_5$  as below:

$$D_5 = u_l f_1(p_5, h_5) \quad (15)$$

using a nonlinear function  $f_1(\cdot, \cdot)$ .

### 3.2.2. Primary attemperators

For primary attemperators, we have

$$D_5 + D_{sw1} = D_4, \quad (16)$$

$$D_5 h_5 + D_{sw1} h_{sw1} = D_4 h_4, \quad (17)$$

$$p_5 \approx p_4. \quad (18)$$

### 3.2.3. Platen superheater

Considering that steam flow at the output of platen superheater cannot be measured, we assume that steam flow at the input of platen superheater is approximately equal to that at the output of platen superheater, namely  $D_4 \approx D_3$ . Therefore, we adopt a lumped parameter at the output of the superheater and energy conservation law to build a model that is

$$\alpha_2 V_3 \frac{d(\rho_3 h_3)}{dt} = D_3(h_4 - h_3) + k_{12}r_B, \quad (19)$$

and  $\alpha_2 = \alpha_2(x_1)$ .

Furthermore, we can get the derivative of enthalpy of steam at the output of platen superheater as follows:

$$c_2 \frac{dh_3}{dt} = D_3(h_4 - h_3) + k_{12}r_B, \quad (20)$$

where  $c_2 = \alpha_2 V_3(h_3 \frac{\partial \rho_3}{\partial h_3} + \rho_3)$ .

**Remark 1.** (20) can be rewritten as:

$$\frac{c_2}{D_3} \frac{dh_3}{dt} + h_3 = \frac{D_5 h_5 (1 + \frac{D_{sw1} h_{sw1}}{D_5 h_5}) + k_{12} r_B}{D_3}. \quad (21)$$

In (21), the inertia time of platen superheater system is  $\frac{c_2}{D_3}$ , and it varies with  $D_3$ . Besides, the ratio,  $\frac{D_{sw1} h_{sw1}}{D_5 h_5}$ , also changes with different loads. When there is a step disturbance on  $D_{sw1}$ , (21) can reflect the its varying system inertia and nonlinearity of platen superheater system in different load conditions.

Differential pressure [16,17] of steam in boiler is

$$\Delta p = g_2(p_m), \quad (22)$$

where  $g_2(\cdot)$  is a nonlinear function, and  $\Delta p = p_m - p_3$  is steam pressure drop in low temperature superheater and platen superheater, MPa. After obtaining  $p_3$  and  $h_3$ , we can calculate the steam temperature at the output of platen superheater,  $T_3$ , °C, which is  $T_1(p_3, h_3)$ , where  $T_1(\cdot, \cdot)$  is a nonlinear function.

### 3.2.4. Secondary attemperators

For secondary attemperators, we have

$$D_3 + D_{sw2} = D_2, \quad (23)$$

$$D_3 h_3 + D_{sw2} h_{sw2} = D_2 h_2, \quad (24)$$

$$p_3 \approx p_2. \quad (25)$$

### 3.2.5. High temperature superheater

According to mass and energy conservation laws, we adopt a lumped parameter at the output of high temperature superheater to establish its model that is

$$V_{st}(\frac{d\rho_{st}}{dt}) = D_2 - D_{st}, \quad (26)$$

$$\alpha_3 V_{st} \frac{d(\rho_{st} h_{st})}{dt} = D_2 h_2 - D_{st} h_{st} + k_{13} r_B, \quad (27)$$

and  $\alpha_3 = \alpha_3(x_1)$ .

Combining (26) and (27), we can get derivatives of enthalpy and pressure of steam at output of high temperature superheater as follows:

$$V_{st}(\frac{\partial \rho_{st}}{\partial p_{st}} \frac{dp_{st}}{dt} + \frac{\partial \rho_{st}}{\partial h_{st}} \frac{dh_{st}}{dt}) = D_2 - D_{st}, \quad (28)$$

$$\alpha_3 V_{st} \{h_{st} \frac{\partial \rho_{st}}{\partial p_{st}} \frac{dp_{st}}{dt} + (h_{st} \frac{\partial \rho_{st}}{\partial h_{st}} + \rho_{st}) \frac{dh_{st}}{dt}\} = D_2 h_2 - D_{st} h_{st} + k_{13} r_B, \quad (29)$$

which can be simplified as

$$b_{31} \frac{dp_{st}}{dt} + b_{32} \frac{dh_{st}}{dt} = D_2 - D_{st}, \quad (30)$$

$$b_{41} \frac{dp_{st}}{dt} + b_{42} \frac{dh_{st}}{dt} = D_2 h_2 - D_{st} h_{st} + k_{13} r_B, \quad (31)$$

where  $b_{31} = V_{st} \frac{\partial \rho_{st}}{\partial p_{st}}$ ,  $b_{32} = V_{st} \frac{\partial \rho_{st}}{\partial h_{st}}$ ,  $b_{41} = \alpha_3 V_{st} h_{st} \frac{\partial \rho_{st}}{\partial p_{st}}$ ,  $b_{42} = \alpha_3 V_{st} (h_{st} \frac{\partial \rho_{st}}{\partial h_{st}} + \rho_{st})$ .

With respect to  $\frac{dp_{st}}{dt}$  and  $\frac{dh_{st}}{dt}$ , (30) and (31) can be transformed to

$$c_{31}(\frac{dp_{st}}{dt}) = (h_2 - d_{21})D_2 + (d_{21} - h_{st})D_{st} + k_{13} r_B, \quad (32)$$

$$c_{32}(\frac{dh_{st}}{dt}) = (h_2 - d_{22})D_2 + (d_{22} - h_{st})D_{st} + k_{13} r_B \quad (33)$$

$$\text{with } c_{31} = b_{41} - \frac{b_{31}b_{42}}{b_{32}}, c_{32} = b_{42} - \frac{b_{32}b_{41}}{b_{31}}, d_{21} = \frac{b_{42}}{b_{32}} \text{ and } d_{22} = \frac{b_{41}}{b_{31}}.$$

**Remark 2.** Similarly, (33) can be rewritten as:

$$\frac{c_{32}}{D_{st}} \frac{dh_{st}}{dt} + h_{st} = \frac{D_3 h_3 (1 + \frac{D_{sw2} h_{sw2}}{D_3 h_3}) + d_{22} (D_{st} - D_3 - D_{sw2}) + k_{13} r_B}{D_{st}}. \quad (34)$$

In (34), the inertia time of platen superheater system is  $\frac{c_{32}}{D_{st}}$ , and it varies with  $D_{st}$ . Besides, the ratio,  $\frac{D_{sw2} h_{sw2}}{D_3 h_3}$ , also changes with different loads. When there is a step disturbance on  $D_{sw2}$ , (34) can reflect the its varying system inertia and nonlinearity of high temperature superheater system in different load conditions.

After obtaining  $p_{st}$  and  $h_{st}$ , we can calculate the main steam temperature,  $T_{st}$ , °C, which is  $T_2(p_{st}, h_{st})$ , where  $T_2(\cdot, \cdot)$  is a nonlinear function.

In practice, feedwater and spray water temperature can influence SST due to variation of heat energy absorbed by steam, and their enthalpy changes with unit load based on data analysis. According to energy conservation, coal flow in furnace,  $r_B$ , is related to unit load directly, and thus feedwater and spray water enthalpy,  $h_{fw}$ ,  $h_{sw1}$  and  $h_{sw2}$  are

$$h_{fw} = h_1(r_B), \quad (35)$$

$$h_{sw1} = h_2(r_B), \quad (36)$$

$$h_{sw2} = h_3(r_B), \quad (37)$$

where  $h_1(\cdot)$ ,  $h_2(\cdot)$  and  $h_3(\cdot)$  are nonlinear functions.

### 3.3. Modeling for turbine system

In turbine system, superheated steam expands in high pressure turbine to generate mechanical work. Similarly, steam from high pressure turbine is reheated in reheaters to expand again in intermediate and low pressure turbines. Steam from low pressure turbine is exhausted to condenser. Additionally, turbine regenerative system is used to heat condensate water so as to enhance boiler efficiency, as shown in Fig. 1.

Main steam flow [38] is defined as

$$D_{st} = \lambda u_t p_{st}^{1-\alpha} \rho_{st}^\alpha, \quad (38)$$

As steam density can be represented as a function of pressure and enthalpy, (38) can be rewritten as

$$D_{st} = u_t f_2(p_{st}, h_{st}) \quad (39)$$

using a nonlinear function  $f_2(\cdot, \cdot)$ .

With help of (39), unit load ( $N_e$ ) can be defined by

$$N_e = \eta [D_{st} h_{st} + D_r(h_{r2} - h_{r1}) - D_{fw} h_{fw}]. \quad (40)$$

Based on mass conservation law, feedwater flow is approximately equal to the main steam flow. Thus, (40) can be rewritten as

$$N_e = \eta [D_{st} (h_{st} - h_{fw}) + D_r(h_{r2} - h_{r1})]. \quad (41)$$

Table 3 presents the ratio of heat energy absorbed by steam in re-heater to the one in boiler section at different conditions of Boiler Maximum Continuous Rating (BMCR).

As shown in Table 3, the ratio decreases monotonically with decreasing of unit load. Coal flow in furnace is directly related to unit load according to energy conservation law. Thus, we have

$$D(r_B) = \frac{D_r(h_{r2} - h_{r1})}{D_{st}(h_{st} - h_{fw})} \quad (42)$$

with a linear function  $D(\cdot)$ .

With help of (42), (41) can be reformulated as

$$N_e = \eta (1 + D(r_B)) D_{st} (h_{st} - h_{fw}), \quad (43)$$

which can be simplified as

$$N_e = k_2 D_{st} (h_{st} - h_{fw}), \quad (44)$$

where  $k_2 = \eta (1 + D(r_B))$ , i.e.,  $k_2 = k(r_B)$ ,  $k(\cdot)$  is a nonlinear function.

Finally, dynamic response of turbine system is faster than that of boiler system, and its inertia is approximately from ten to thirty seconds. Considering the effect of inertia, (44) can be redefined as

$$\frac{dN_e}{dt} = \frac{1}{c_4} k_2 D_{st} (h_{st} - h_{fw}) - \frac{1}{c_4} N_e \quad (45)$$

with inertia time in turbine system,  $c_4$ , s.

**Remark 3.** As shown in (44),  $k_2$  is related with coal flow in furnace. If defining  $k_2 = k(p_m)$  in [17], throttle valve may reduce opening for improving unit load due to the increase of steam pressure. This violates energy conservation law that unit load changes with coal flow in furnace. Thus, it is appropriate to define  $k_2 = k(r_B)$ .

### 3.4. Summary

According to above analysis, the model structure of OTBT coal-fired units can be summarized in form of following state space equation as:

$$\dot{X} = A(X) + B(X, U), \quad (36)$$

$$Y = C(X), \quad (37)$$

$$\begin{cases} \dot{X} = A(X) + B(X, U), \\ Y = C(X), \end{cases} \quad (46)$$

or in a more detailed form of

$$\begin{aligned} \dot{x}_1 &= -\frac{1}{c_0} x_1 + \frac{e^{-ts}}{c_0} u_1, \\ \dot{x}_2 &= \left(\frac{h_{fw} - d_{11}}{c_{11}}\right)(u_2 - u_4 - u_5) + \left(\frac{d_{11} - h_5}{c_{11}}\right) f_1(x_2 - g(x_2), h_5) u_3 + k_{11} \frac{x_1}{c_{11}}, \\ \dot{x}_3 &= \left(\frac{h_{fw} - d_{12}}{c_{12}}\right)(u_2 - u_4 - u_5) + \left(\frac{d_{12} - h_5}{c_{12}}\right) f_1(x_2 - g(x_2), h_5) u_3 + k_{11} \frac{x_1}{c_{12}}, \\ \dot{x}_4 &= \frac{D_3(h_4 - x_4)}{c_2} + k_{12} \frac{x_1}{c_2}, \\ \dot{x}_5 &= \left(\frac{h_2 - d_{21}}{c_{31}}\right) D_2 + \left(\frac{d_{31} - x_6}{c_{31}}\right) f_2(x_5, x_6) u_3 + k_{13} \frac{x_1}{c_{31}}, \\ \dot{x}_6 &= \left(\frac{h_2 - d_{22}}{c_{32}}\right) D_2 + \left(\frac{d_{32} - x_6}{c_{32}}\right) f_2(x_5, x_6) u_3 + k_{13} \frac{x_1}{c_{32}}, \\ \dot{x}_7 &= -\frac{x_7}{c_4} + \frac{k_2(x_6 - h_{fw}) f_2(x_5, x_6) u_3}{c_4}, \end{aligned}$$

$$h_{fw} = h_1(x_1), h_{sw1} = h_2(x_1), h_{sw2} = h_3(x_1), h_5 = kx_3, p_5 = x_2 - g_1(x_2), p_3$$

$$= x_2 - g_2(x_2),$$

$$D_5 = f_1(p_5, h_5) u_3, D_4 = D_5 + u_4, h_4 = \frac{D_5 h_5 + u_4 h_{sw1}}{D_4}, D_3 = D_4, D_2 \\ = D_3 + u_5, h_2 = \frac{D_3 h_3 + u_5 h_{sw2}}{D_2},$$

$$y_1 = x_5,$$

$$y_2 = x_3,$$

$$y_3 = x_7,$$

$$y_4 = T_1(x_2, x_4),$$

$$y_5 = T_2(x_5, x_6),$$

$$\text{where } U = [u_1, u_2, u_3, u_4, u_5]^T = [u_B, D_{fw}, u_t, D_{sw1}, D_{sw2}]^T; Y =;$$

$$[y_1, y_2, y_3, y_4, y_5]^T = [p_{st}, h_m, N_e, T_3, T_{st}]^T$$

$$X = [x_1, x_2, x_3, x_4, x_5, x_6, x_7]^T = [r_B, p_m, h_m, h_3, p_{st}, h_{st}, N_e]^T;$$

### 3.5. Control structure

When the physical structure of the model established is obtained, the control structure based on the model should be discussed, as in the diagram shown in Fig. 3. As shown in Fig. 3, when load command needs to be raised up, control inputs  $u_1$ ,  $u_2$  and  $u_3$  accordingly change with the load command. The control valve input  $u_3$  enlarges to release heat energy stored in boiler in order to make OTBT units track load command quickly, and the fuel input  $u_1$  increases immediately to provide more heat energy in the furnace. Besides, the feedwater input  $u_2$  also requires to be raised in order to provide qualified steam and maintain safe operation of the units. Due to varying coal quality, steam pressure may not reach its set value. Considering that  $u_3$  can change the steam pressure  $p_{st}$  quickly,  $u_3$  should cooperate with  $u_1$  to reduce the error of  $p_{st}$ . In order to remain stability of  $h_m$ , feedwater flow,  $D_{fw}$ , should be changed quickly to maintain  $h_m$  at a rational range. For superheater, the task of primary spray water,  $D_{sw1}$ , is to protect platen superheater and control the temperature of superheated steam at the output of platen superheater,  $T_{pout}$ , to be within a safe range. Similarly, the secondary spray water,  $D_{sw2}$ , is to maintain superheated steam temperature,  $T_{st}$ , at a set value, and enhance the operational safety and thermal efficiency of

**Table 3**

Ratio of  $D_r(h_{r2} - h_{r1})$  to  $D_{st}(h_{st} - h_{fw})$  at different conditions of BMCR.

Condition	$\frac{D_r(h_{r2} - h_{r1})}{D_{st}(h_{st} - h_{fw})}$
100%BMCR	0.211
75%BMCR	0.192
50%BMCR	0.170
30%BMCR	0.155

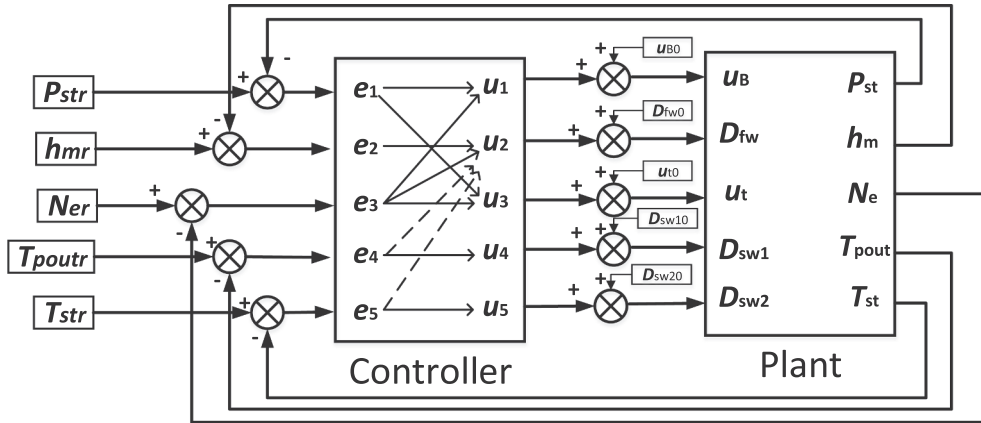


Fig. 3. A diagram of control structure of CCS and SST system for OTBT units based on the model. Solid line: a variable can change one variable; dashed line: a variable may change one variable.

OTBT units. If spray water flow exceeds its maximum value, feedwater flow,  $D_{fw}$ , should change to adjust intermediate-point enthalpy,  $h_m$ , to reduce spray water flow. Above control structure and mechanism analysis can contribute to controller design based on this model.

#### 4. Parameter identification

In the OTBT model (46), there are eight static parameters,  $k_{11}$ ,  $k_{12}$ ,  $k_{13}$ ,  $k_2$ ,  $l$ ,  $h_{fw}$ ,  $h_{sw1}$  and  $h_{sw2}$ , twelve dynamic parameters,  $\tau$ ,  $c_0$ ,  $c_{11}$ ,  $c_{12}$ ,  $d_{11}$ ,  $d_{12}$ ,  $c_2$ ,  $c_{31}$ ,  $c_{32}$ ,  $d_{21}$ ,  $d_{22}$  and  $c_4$ , and six functions,  $f_1(\cdot, \cdot)$ ,  $f_1(\cdot, \cdot)$ ,  $f_2(\cdot, \cdot)$ ,  $g_1(\cdot)$ ,  $T_1(\cdot, \cdot)$ , and  $T_2(\cdot, \cdot)$  that needs to be identified in this section.

##### 4.1. Identification of static parameters

In steady-state conditions, (5), (6), (7), (19), (26) and (27) result in

$$0 = u_B^* - r_B^*, \quad (47)$$

$$0 = D_{fw}^* - D_{sw1}^* - D_{sw2}^* - D_5^*, \quad (48)$$

$$0 = (D_{fw}^* - D_{sw1}^* - D_{sw2}^*)h_{fw}^* - D_5^*h_5^* + k_{11}r_B^*, \quad (49)$$

$$0 = D_3^*(h_4^* - h_3^*) + k_{12}r_B^*, \quad (50)$$

$$0 = D_2^* - D_{st}^*, \quad (51)$$

$$0 = D_2^*h_2^* - D_{st}^*h_{st}^* + k_{13}r_B^*, \quad (52)$$

where superscript \* means variables lie in steady states.

Combined with (47)–(52) and (45), (16), (17), (24), static parameters can be calculated by

$$l = \frac{h_5^*}{h_m^*}, \quad (53)$$

$$k_{11} = \frac{D_5^*h_5^* - (D_{fw}^* - D_{sw1}^* - D_{sw2}^*)h_{fw}^*}{u_B^*}, \quad (54)$$

$$k_{12} = \frac{(D_5^* + D_{sw1}^*)h_3^* - D_5^*h_5^* - D_{sw1}^*h_{sw1}^*}{u_B^*}, \quad (55)$$

$$k_{13} = \frac{D_{st}^*h_{st}^* - D_{sw2}^*h_{sw2}^* - (D_{sw1}^* + D_5^*)h_3^*}{u_B^*}, \quad (56)$$

$$k_2 = \frac{N_e^*}{D_{st}^*(h_{st}^* - h_{fw}^*)}, \quad (57)$$

in which variables at different steady-state loads are listed in Table 4.

To guarantee model accuracy, it is necessary to estimate static parameters accurately. Static parameters can be calculated by using steady-state data and (53)–(57), and results are shown in Table 5.

We can see from Table 5 that  $l$ ,  $k_{11}$ ,  $k_{12}$ ,  $k_{13}$  and  $k_2$  change with unit load in a roughly clear way, and thus these parameters can be identified based on steady-state running data and nonlinear regression analysis. Static parameters can be given as below:

Table 4  
Steady-state data at different loads.

$u_B/(\text{kg}\cdot\text{s}^{-1})$	$D_{fw}/(\text{kg}\cdot\text{s}^{-1})$	$u_t/(\%)$	$D_{sw1}/(\text{kg}\cdot\text{s}^{-1})$	$D_{sw2}/(\text{kg}\cdot\text{s}^{-1})$	$h_{fw}/(\text{kJ}\cdot\text{kg}^{-1})$	$h_m/(\text{kJ}\cdot\text{kg}^{-1})$	$p_m/(\text{MPa})$	$D_5/(\text{kg}\cdot\text{s}^{-1})$	$h_5/(\text{kJ}\cdot\text{kg}^{-1})$
$p_s/(\text{MPa})$	$h_{sw}/(\text{kJ}\cdot\text{kg}^{-1})$	$h_3/(\text{kJ}\cdot\text{kg}^{-1})$	$p_3/(\text{MPa})$	$T_3/(\text{°C})$	$D_{st}/(\text{kg}\cdot\text{s}^{-1})$	$p_{st}/(\text{MPa})$	$h_{st}/(\text{kJ}\cdot\text{kg}^{-1})$	$T_{st}/(\text{°C})$	$N_e/(\text{MW})$
56.5	401.9	68.41	1.546	0.165	1118.0	2834.7	15.6	405.5	3061.7
67.2	455.9	67.13	2.581	1.761	1164.5	2886.4	18.4	455.6	3183.1
95.7	667.1	67.04	8.695	23.565	1262.6	2791.2	25.1	639.6	3074.6
102.6	721.8	66.66	8.099	21.545	1280.8	2791.0	27.6	702.4	3052.2
116.8	800.3	67.70	10.497	24.539	1308.5	2735.6	30.9	780.3	2987.6
13.9	1130.6	3293.5	12.9	483.9	408.8	13.1	3486.5	556.2	496.5
16.5	1178.4	3425.4	10.6	522.5	466.7	15.6	3571.6	597.7	600.8
24.0	1261.3	3290.2	20.3	516.5	669.5	22.8	3522.3	602.9	878.6
26.1	1280.8	3294.1	22.8	527.9	724.7	24.7	3504.6	602.9	951.2
28.4	1304.5	3229.1	26.8	524.2	802.8	26.9	3485.3	602.9	1047.9

**Table 5**  
Static parameters under different load conditions.

Load/(MW)	Static parameters				
	$k_{11}$	$k_{12}$	$k_{13}$	$k_2$	$l$
496.5	14048	1721.8	1492.9	0.5128	1.0801
600.8	14183	1782.7	1462.1	0.5348	1.1028
878.6	12175	1624.9	2042.6	0.5807	1.1015
951.2	12252	1814.2	1674.5	0.5902	1.0936
1047.9	11386	1786.2	1817.4	0.5996	1.0922

$$\begin{aligned}
 l &= -0.000016739r_B^2 + 0.00294744r_B + 0.973044, \\
 h_{fw} &= 471.67r_B^{0.215}, h_{sw1} = h_{sw2} = 522.57r_B^{0.193}, \\
 k_{11} &= -0.10233r_B^2 - 30.144r_B + 16277, k_{12} = 0.07672r_B^2 - 12.66r_B \\
 &\quad + 2225.945, \\
 k_{13} &= -0.2143r_B^2 + 43.31r_B - 338.57, k_2 = -1.5422 * 10^{-5}r_B^2 + 4.093 \\
 &\quad * 10^{-3}r_B + 0.33177.
 \end{aligned}$$

#### 4.2. Estimation of nonlinear functions

Based on steady-state running data, it is easy to obtain the functions  $\Delta p = g_1(p_m)$  and  $\Delta p = g_2(p_m)$ , that are

$$\begin{aligned}
 \Delta p = g_1(p_m) &= 0.01784p_m^2 - 0.8p_m + 10.0919, \Delta p = g_2(p_m) \\
 &= -0.04112p_m^2 + 1.867p_m - 15.018.
 \end{aligned}$$

Notice that  $D_{st} = u_{st}f(p_{st}, h_{st})$  and  $D_5 = u_5f(p_5, h_5)$  were used to calculate the main steam flow and the steam flow at the output of low temperature superheater, respectively. After many trials, we define  $f(p, h) = \theta p / (\phi h + \psi)$  with constants  $\theta, \phi$  and  $\psi$ , and the functions of steam flow are identified based on large-scale running data as

$$f_1(p_{st}, h_{st}) = \frac{91611p_{st}}{0.76h_{st} - 592.95}, f_2(p_5, h_5) = \frac{889857p_5}{6.29h_5 + 2862.86}.$$

To calculate steam temperature,  $T_3$  and  $T_{st}$ , bilinear fitting method is adopted, and we define

$$T_1(p_5, h_5) = \kappa_1 p_5^2 + \beta_1 p_5 + \gamma_1, \quad (58)$$

$$T_2(p_{st}, h_{st}) = \kappa_2 p_{st}^2 + \beta_2 p_{st} + \gamma_2, \quad (59)$$

where  $\kappa_1, \beta_1$  and  $\gamma_1$  are all the functions of  $h_5$ , and  $\kappa_2, \beta_2, \gamma_2$  are all the functions of  $h_{st}$ . They are identified as

$$\begin{aligned}
 \kappa_1 &= -1.292 * 10^{-7}h_5^2 + 0.0009804h_5 - 1.878, \\
 \beta_1 &= 6.5093 * 10^{-6}h_5^2 - 0.0524h_5 + 108.138, \\
 \gamma_1 &= 1.8054 * 10^{-5}h_5^2 + 0.335h_5 - 887.064, \\
 \kappa_2 &= -1.15034 * 10^{-7}h_{st}^2 + 0.0008784h_{st} - 1.6941, \\
 \beta_2 &= 6.31422 * 10^{-6}h_{st}^2 - 0.0509h_{st} + 105.32, \\
 \gamma_2 &= 3.9667 * 10^{-6}h_{st}^2 + 0.4311h_{st} - 1050.743.
 \end{aligned}$$

#### 4.3. Optimization of dynamic parameters

After identifying static parameters and functions, dynamic parameters will be optimized by immune genetic algorithm (IGA) [17]. Large-scale running data are sampled from a USC OTBT coal-fired unit at the interval of one second. As there are twelve dynamic parameters required to be identified in this study, we divide the parameters into two groups rather than a whole one in order to improve the accuracy.

Step 1: The first group of dynamic parameters is  $\theta_1 = \{\tau, c_0, c_{11}, c_{12}, c_2, d_{11}, d_{12}\}$ . Based on the running data, we aim to minimize the error criterion,  $E_1$ , defined by

$$\begin{aligned}
 E_1 = \min_{\theta_1} \sum_{i=1}^N & \left( \frac{|p_{m,r}(i) - p_m(i)|}{p_{m,r}(i)} + \frac{|h_{m,r}(i) - h_m(i)|}{h_{m,r}(i)} + \frac{|D_{5,r}(i) - D_5(i)|}{D_{5,r}(i)} \right. \\
 & \left. + \frac{|T_{3,r}(i) - T_3(i)|}{T_{3,r}(i)} \right), \\
 \text{subject to } \dot{x} &= f_3(x, u, \theta_1), x(0) = x_0, y = h_1(x, \theta_1).
 \end{aligned}$$

Step 2: After obtaining the first group of dynamic parameters, the next group of dynamic parameters is  $\theta_2 = \{c_{31}, c_{32}, d_{21}, d_{22}, c_4\}$ . Similarly, we define  $E_2$  as

$$\begin{aligned}
 E_2 = \min_{\theta_2} \sum_{i=1}^N & \left( \frac{|p_{st,r}(i) - p_{st}(i)|}{p_{st,r}(i)} + \frac{|T_{st,r}(i) - T_{st}(i)|}{T_{st,r}(i)} + \frac{|N_{e,r}(i) - N_e(i)|}{N_{e,r}(i)} \right), \\
 \text{subject to } \dot{x} &= f_4(x, u, \theta_2), x(0) = x_0, y = h_2(x, \theta_2),
 \end{aligned}$$

where  $(\cdot)(i)$  represents the calculated values of corresponding variables, and  $(\cdot)_r(i)$  is the measured values of relevant variables.  $\theta_1$  and  $\theta_2$  are the dynamic parameters needed to be identified, and  $x_0$  is the initial value of state variables.  $f_1(\cdot), h_1(\cdot), f_2(\cdot)$  and  $h_2(\cdot)$  are nonlinear functions, and  $N$  is the total number of groups of running data.

To further improve model accuracy, this paper proposes to model correction factors of heat energy absorbed by steam, and the ratio of coal flow command to feedwater flow (i.e.,  $\frac{u_B}{D_{fw}}$ ), is used to establish the dynamic models. Besides, there exists inertia time between coal flow command,  $u_B$  and coal flow in furnace,  $r_B$ , and then we use a first-order inertia section and a quadratic function as its model structure, i.e.,

$$\dot{H}(t) = \frac{1}{d}(-H(t) + a(\frac{u_B(t)}{D_{fw}(t)})^2 + b\frac{u_B(t)}{D_{fw}(t)} + c). \quad (60)$$

Lastly, operational data and optimization method, IGA [17] are combined to search for many groups of parameters under different operating ranges, and specific procedure is presented as follows:

Step 1: Improve accuracy of steam enthalpy in separator,  $h_m$ . After obtaining twelve dynamic parameters, we aim to optimize many groups of dynamic parameters under different load ranges,  $\theta_3 = \{a_{hm}, b_{hm}, c_{hm}, d_{hm}\}$ , by defining  $E_3$  as

$$\begin{aligned}
 E_3 = \min_{\theta_3} \sum_{i=1}^{N_1} & \left( \frac{|h_{m,r}(i) - h_m(i)|}{h_{m,r}(i)} \right), \\
 \text{subject to } \dot{H}(t) &= f_5(\frac{u_B(t)}{D_{fw}(t)}, H(t), \theta_3), H(0) = 1, y(t) = H(t),
 \end{aligned}$$

where  $N_1$  is total number of a group of running data.

Step 2: Improve accuracy of steam temperature at the output of platen superheater,  $T_3$ . After improving accuracy of steam enthalpy in separator, we aim to optimize many groups of dynamic parameters under different load ranges,  $\theta_4 = \{a_{T3}, b_{T3}, c_{T3}, d_{T3}\}$ , by defining  $E_4$  as

$$\begin{aligned}
 E_4 = \min_{\theta_4} \sum_{i=1}^{N_2} & \left( \frac{|T_{3,r}(i) - T_3(i)|}{T_{3,r}(i)} \right), \\
 \text{subject to } \dot{H}(t) &= f_6(\frac{u_B(t)}{D_{fw}(t)}, H(t), \theta_4), H(0) = 1, y(t) = H(t).
 \end{aligned}$$

Step 3: Improve accuracy of superheated steam temperature, main steam pressure and unit load, (i.e.,  $T_{st}, p_{st}$  and  $N_e$ ). After Step 1 and Step 2, we aim to optimize many groups of dynamic parameters under different load ranges,  $\theta_5 = \{a_{Tst}, b_{Tst}, c_{Tst}, d_{Tst}\}$ , by defining  $E_5$  as

**Table 6**

Calculated values and relative errors at different steady-state loads.

Calculated values					Relative errors (%)				
$p_{st}$ /MPa	$h_m$ /(kg·s <sup>-1</sup> )	$N_e$ /MW	$T_3$ /°C	$T_{st}$ /°C	$\delta p_{st}$	$\delta h_m$	$\delta N_e$	$\delta T_3$	$\delta T_{st}$
13.2	2852.8	488.9	484.3	557.7	0.76	0.64	1.53	0.08	0.27
15.8	2882.7	591.3	525.2	601.0	1.28	0.13	1.58	0.52	0.55
22.7	2797.7	884.0	518.1	606.2	0.44	0.23	0.61	0.31	0.55
24.5	2786.7	948.9	528.4	602.4	0.81	0.15	0.24	0.09	0.08
26.6	2737.3	1045.0	522.9	603.4	1.12	0.08	0.28	0.25	0.08

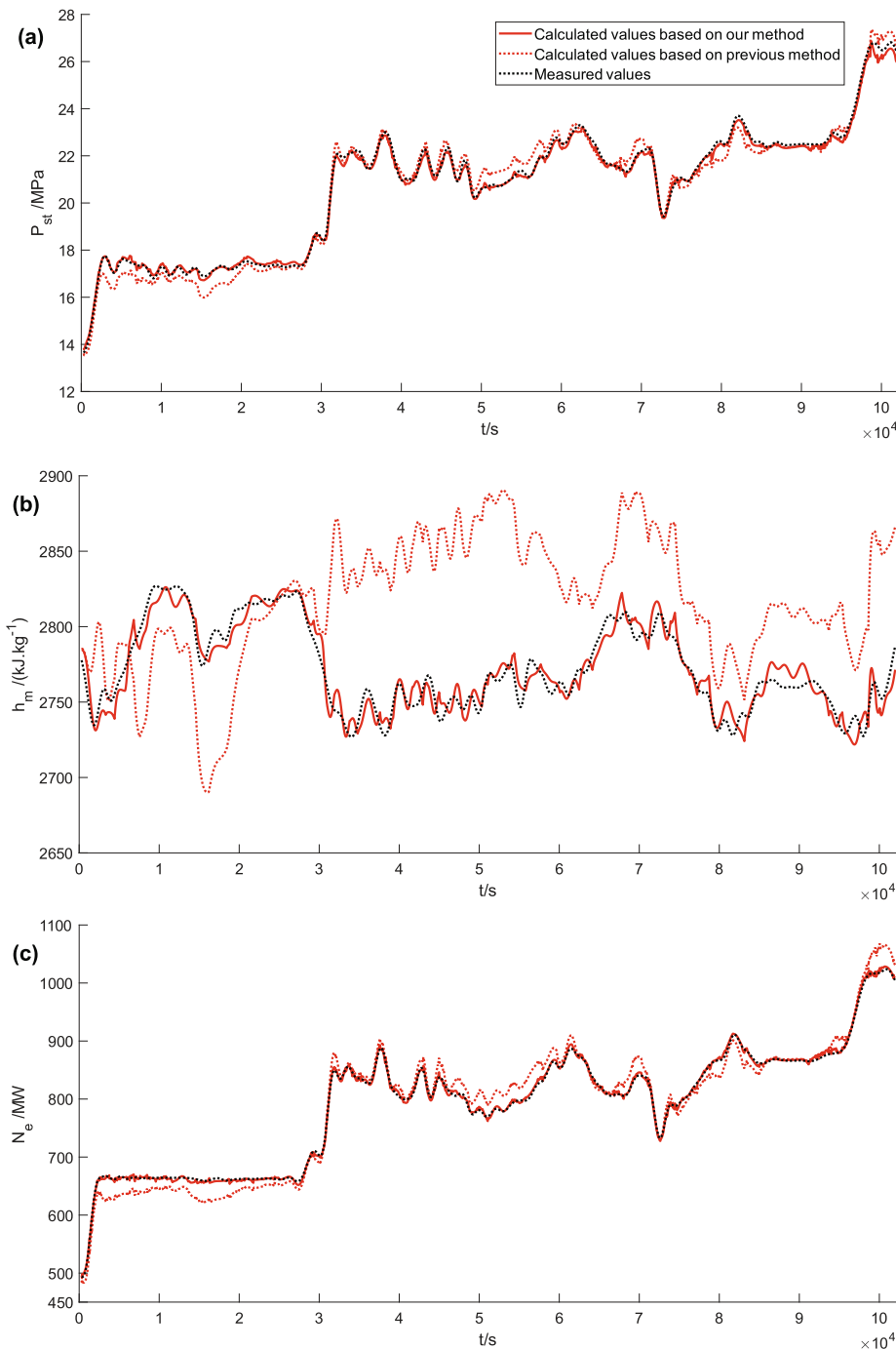


**Fig. 4.** Compared and measured responses of outputs in Case A. (a) Responses of main steam pressure, (b) Responses of steam enthalpy in separator, (c) Responses of unit load, (d) Responses of steam temperature at the output of platen superheater, (e) Responses of SST.

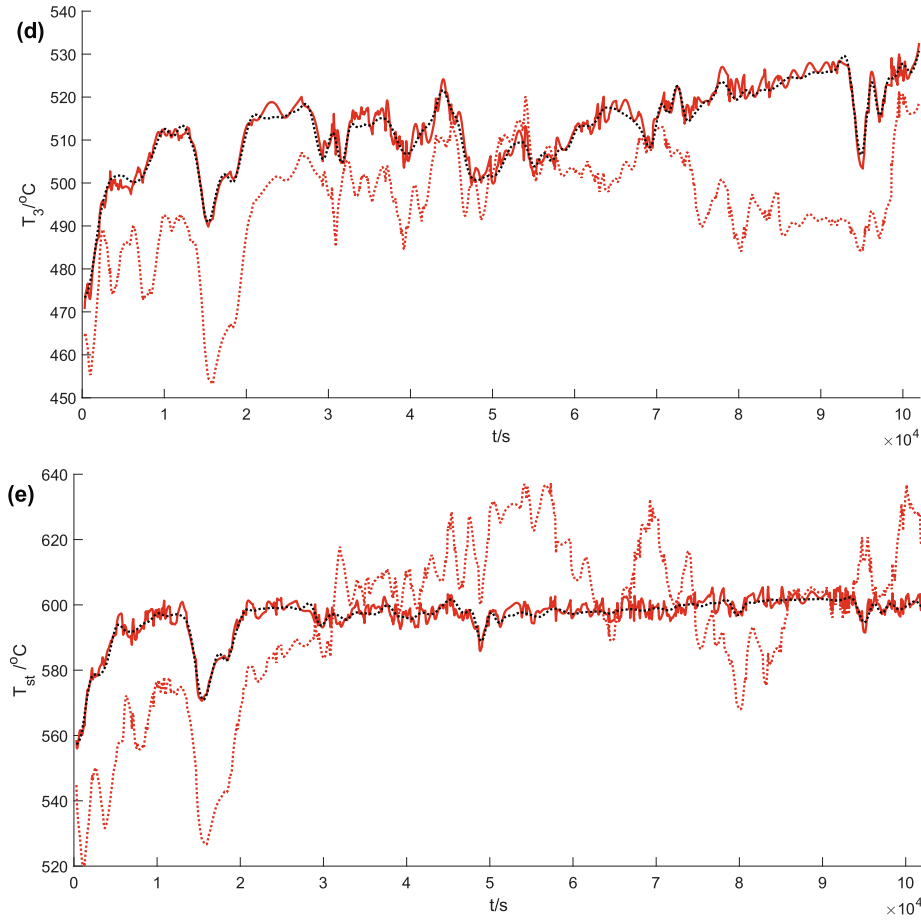


Fig. 4. (continued)

$$E_5 = \min_{\theta_5} \sum_{i=1}^{N_1} \left( \frac{|T_{st,r}(i) - T_{st}(i)|}{T_{st,r}(i)} + \frac{|p_{st,r}(i) - p_{st}(i)|}{p_{st,r}(i)} + \frac{|N_{e,r}(i) - N_e(i)|}{N_{e,r}(i)} \right),$$

subject to  $\dot{H}(t) = f_7\left(\frac{u_B(t)}{D_{fw}(t)}, H(t), \theta_5\right)$ ,  $H(0) = 1$ ,  $y(t) = H(t)$ .

where  $f_5(\cdot)$ ,  $f_6(\cdot)$  and  $f_7(\cdot)$  are nonlinear functions (60).

After implementing the optimization, dynamic parameters are  $\tau = 12$ ,  $c_0 = 152$ ,  $c_{11} = 110475$ ,  $c_{12} = 197128$ ,  $d_{11} = 103$ ,  $d_{12} = 2004$ ,  $c_2 = 89912$ ,  $c_{31} = 2667932$ ,  $c_{32} = 44805$ ,  $d_{21} = 236$ ,  $d_{22} = 3001$ ,  $c_4 = 10$ ,

and many groups of parameters in the models of correction factor are also presented in Appendix A. Then the ranges of five inputs are:

$$u_B \in [50 \text{ kg/s}, 120 \text{ kg/s}], D_{fw} \in [350 \text{ kg/s}, 850 \text{ kg/s}], u_t \in [0.6, 0.7], D_{sw1} \in [0, 3\%D_{fw}], D_{sw2} \in [0, 3\%D_{fw}].$$

## 5. Validations

### 5.1. Steady-state validation

In this section, steady-state validation was performed based on our model considering correction factors. Those factors in steady-state conditions from 496.5 MW to 1047.9 MW are given, and Table 6 shows calculated values and relative errors.

$$Correct_{hm} = [0.9822 \ 0.971 \ 0.972 \ 0.9956 \ 0.9621];$$

$$Correct_{T3} = [0.8888 \ 1.022 \ 1.0103 \ 1.0475 \ 1.085];$$

$$Correct_{Tst} = [0.9036 \ 0.7678 \ 1.0986 \ 0.9852 \ 1.1419].$$

It can be seen from Table 6 that the minimum and maximum relatively

errors are 0.08 % and 1.58 %, respectively, which indicates that the model has satisfactory steady-state accuracies at steady-state conditions from 496.5 MW to 1047.9 MW.

### 5.2. Dynamic validation of closed-loop operating data

In this section, two sets of widely load-changing running data with different trends were used for dynamic validation, and two sets of running data are entitled Case A and Case B, respectively. Unit load varies from 495.2 MW to 1030.3 MW in Case A, and unit load varies from 1055.4 MW to 486.7 MW in Case B. Due to different operational conditions in Case B, some nonlinear functions, such as heat energy absorbed by steam, need to be identified again, and those functions are provided as follows:

$$l = -0.000031052r_B^2 + 0.00440113r_B + 0.9489, k_{11} = 0.739r_B^2 - 163.51r_B + 20874.3,$$

$$k_{12} = -0.4977r_B^2 + 73.6r_B - 1012.7, k_{13} = 0.449r_B^2 - 45.28r_B + 2569.2.$$

Relevant results are shown in Figs. 4 and 5, and Table 7 shows mean relative errors (MREs) and root mean square errors (RMSEs) of output variables.

After referring to the work [32], different operational conditions, such as varying coal quality and combustion process, are considered in this work, and importantly heat energy absorbed from coal burning is corrected carefully. As shown in Figs. 4 and 5 and Table 7, calculated values of model outputs based on the proposed method are in strongly accordance with the measured values by comparing calculated values based on previous methods. In above table, maximum mean relative error of our model outputs is 0.56 %, and the minimum is 0.20 %. It indicates that dynamic models of correction factors proposed in our

study can correct steam heat absorbed from coal burning effectively to improve model accuracy by combining dynamic operational data and optimization algorithm. By comparison in Table 7, mean relative errors and root mean square errors of outputs are reduced by at least 50% in cases both A and B, and thus our model has higher accuracy. From above results, model outputs based on previous optimization methods [16,17,32] cannot achieve satisfactory accuracies due to the following reasons:

*Reason for analysis:*

1. In practical operation, running data in a wide load range do not contain enough steady-state data, which means that static

parameters and functions based on steady-state data simply describe rough fitting relationships between variables under dynamic operation.

2. Dynamic running data in a wide load range are utilized to optimize a set of dynamic parameters, and the parameters simply guarantee a minimum sum of relative errors of all output variables. Therefore, accuracy of every output may not be satisfactory by using this optimization method.

To solve those problems, we model correction factors to improve accuracy of steam energy functions (i.e.,  $k_{11}$ ,  $k_{12}$  and  $k_{13}$ ) by combining dynamic running data and IGA [17] under different operational ranges.

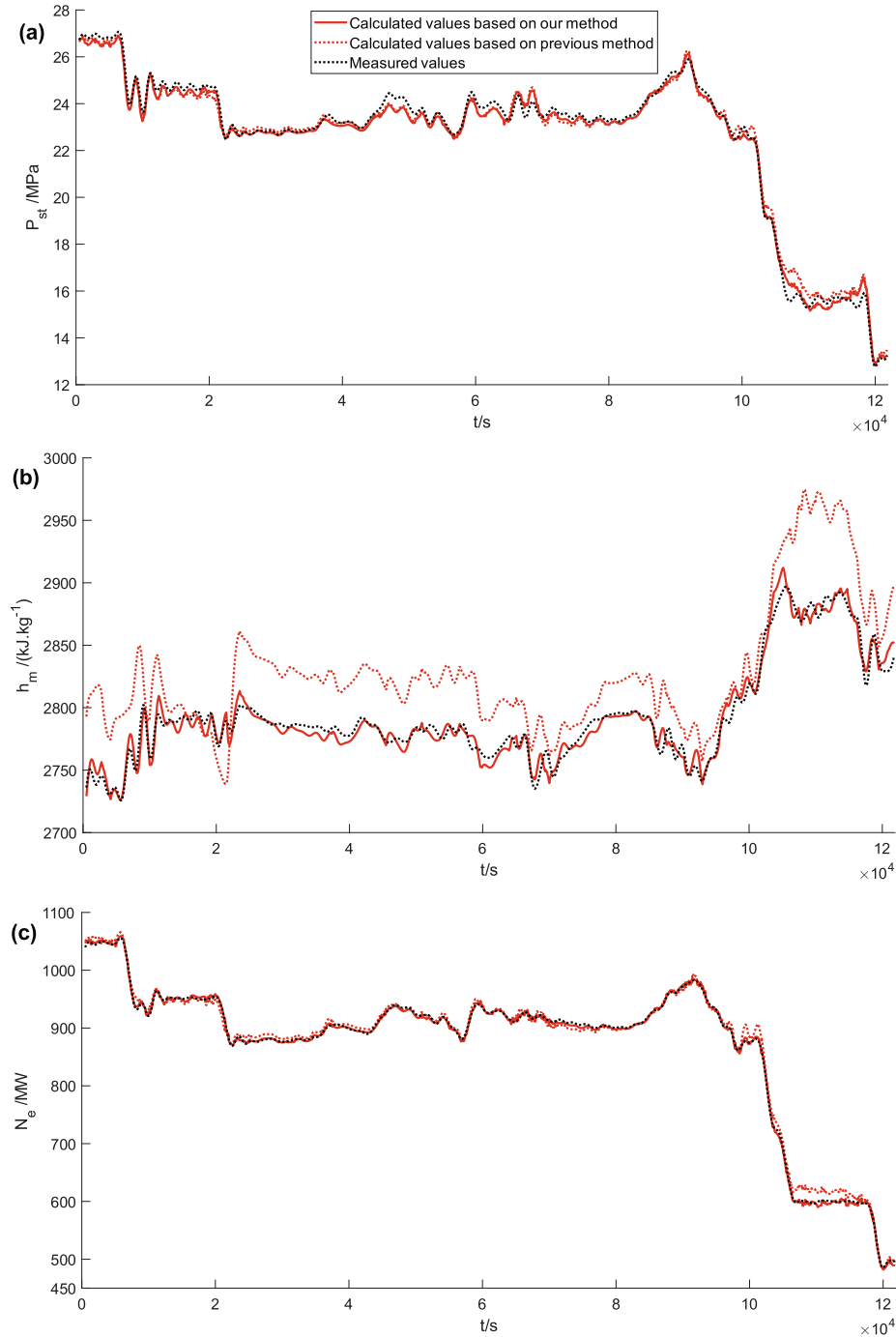


**Fig. 5.** Compared and measured responses of outputs in Case B. (a) Responses of main steam pressure, (b) Responses of steam enthalpy in separator, (c) Responses of unit load, (d) Responses of steam temperature at the output of platen superheater, (e) Responses of SST.

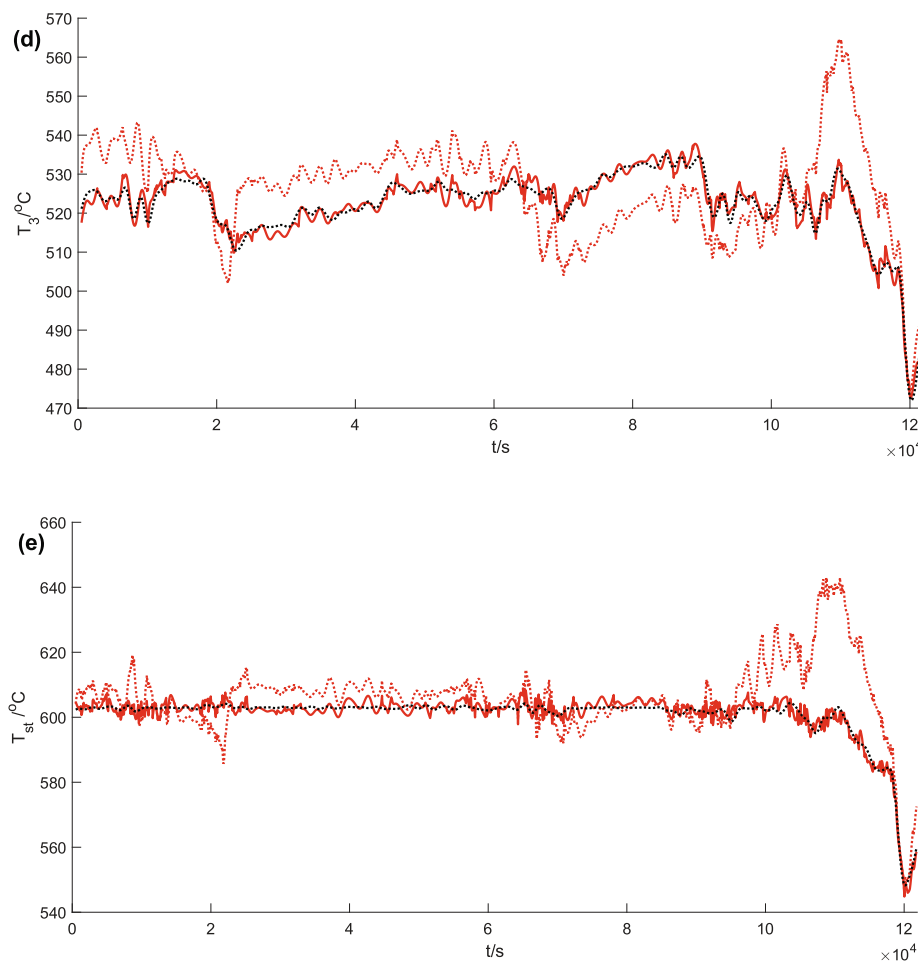


Fig. 5. (continued)

Thus, model accuracy can be further improved due to full use of dynamic running data. This method considers the influence of varying coal quality and combustion process, and can remedy modeling errors effectively. In future, the model based on this optimization method can be used for online prediction, and least square algorithm or other algorithms may further improve model accuracy while costing less computational time online.

### 5.3. Open-loop simulation and analysis

In this section, some simulations were conducted to analyze the open-loop performance of proposed model. The open-loop responses are shown in Figs. 6–10, and characteristics of open-loop responses are analyzed as below.

Fig. 6 shows responses to a step increase of coal flow command. When coal flow command increases abruptly by 14 kg/s, output

variables gradually increase after time delay of 15s. Main steam pressure,  $P_{st}$ , gradually increases from 13.21 MPa to 15.95 MPa due to increasing heat energy, and its time constant is 358s. As feedwater flow keeps unchanged, steam enthalpy and temperature, namely,  $h_m$ ,  $T_3$  and  $T_{st}$ , slowly rise from 2852.8 kJ/kg, 484.3 °C and 557.7 °C to 3218.1 kJ/kg, 676.8 °C and 796.1 °C, respectively, and their time constants are 905s, 1085s and 1139s, respectively. Similarly, unit load gradually increases from 491.3 MW to 631.1 MW, and its time constant is 398s.

Fig. 7 shows responses to a step increase of feedwater flow. When feedwater flow rises abruptly by 40 kg/s, steam in tubes gets squeezed, and output variables start to vary after time delay of 3s. Due to the squeezing effect, main steam pressure increases quickly from 13.21 MPa to 13.73 MPa, and then gradually decreases to 13.38 MPa on account of unchanged coal flow command. Similarly, unit load raises from 491.3 MW to 510.1 MW at once, and gradually restores to the

Table 7

Mean relative errors and root mean square errors of output variables.

Method		$P_{st}$ /MPa	$h_m$ /kJ·kg <sup>-1</sup>	$N_e$ /MW	$T_3$ / °C	$T_{st}$ / °C
Model with correction factor in Case A	MRE(%)	0.54	0.26	0.35	0.30	0.26
	RMSE	0.14	8.40	3.50	1.90	1.86
Previous optimization method in Case A	MRE(%)	1.58	2.22	2.17	3.41	3.02
	RMSE	0.39	70.26	20.04	20.47	21.79
Model with correction factor in Case B	MRE(%)	0.56	0.20	0.36	0.29	0.25
	RMSE	0.15	6.98	3.51	1.86	1.82
Previous optimization method in Case B	MRE(%)	1.12	1.32	0.82	2.02	1.25
	RMSE	0.31	41.73	8.68	12.23	11.32

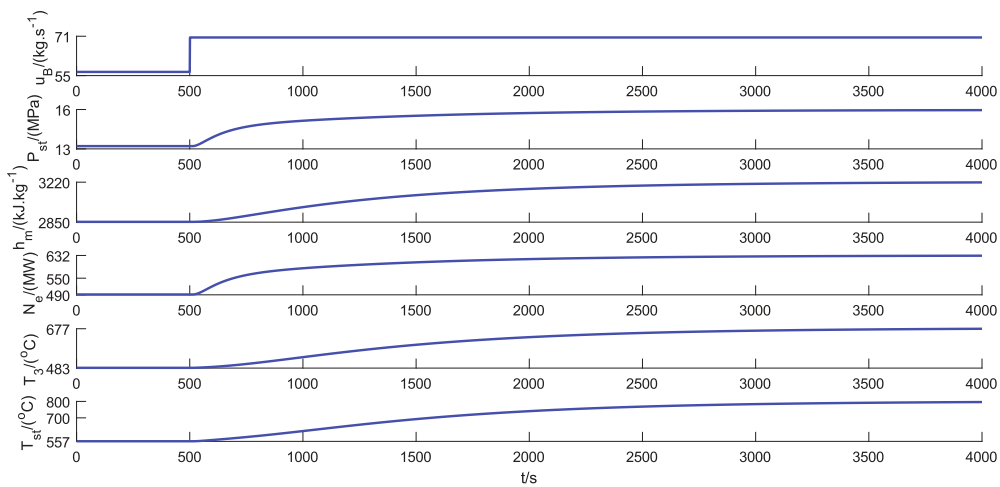


Fig. 6. Step responses of the OTBT model to coal flow command.

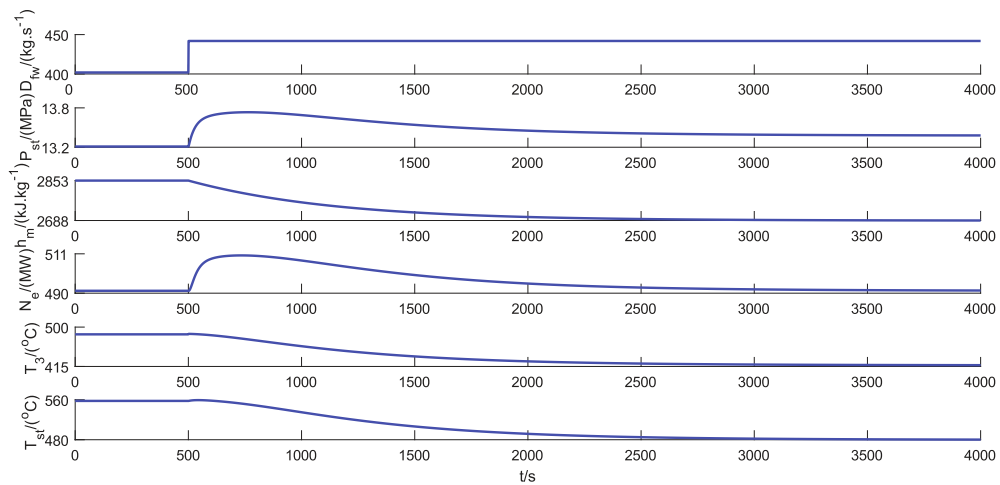


Fig. 7. Step responses of the OTBT model to feedwater flow.

original level. As coal flow in furnace keeps unchanged, steam temperature and enthalpy gradually decrease from 2852.8 kJ/kg, 484.3 °C and 557.7 °C to 2688.1 kJ/kg, 417.8 °C and 480.2 °C, respectively, and then their time constants are 632s, 838s and 949s, respectively.

Fig. 8 shows responses to a step increase of throttle valve opening. When the opening promptly increases by 5 %, output variables vary after time delay of 2s. Main steam pressure,  $P_{st}$ , quickly declines from

13.21 MPa to 12.31 MPa due to enlarged flow area, where its time constant is 26s. Similarly, steam temperatures,  $T_3$ , declines from 484.3 °C to 483.5 °C, due to the rapid change of  $P_{st}$ , where time constant is 9s. Due to the rapid change of  $P_{st}$ ,  $T_{st}$  declines quickly from 557.7 °C to 552.4 °C, and gradually raises to 554.2 °C after releasing heat stored in boiler. For steam enthalpy,  $h_m$ , the change of  $P_{st}$  has a slight influence on  $h_m$  due to heat energy stored in boiler, and  $h_m$  decreases from

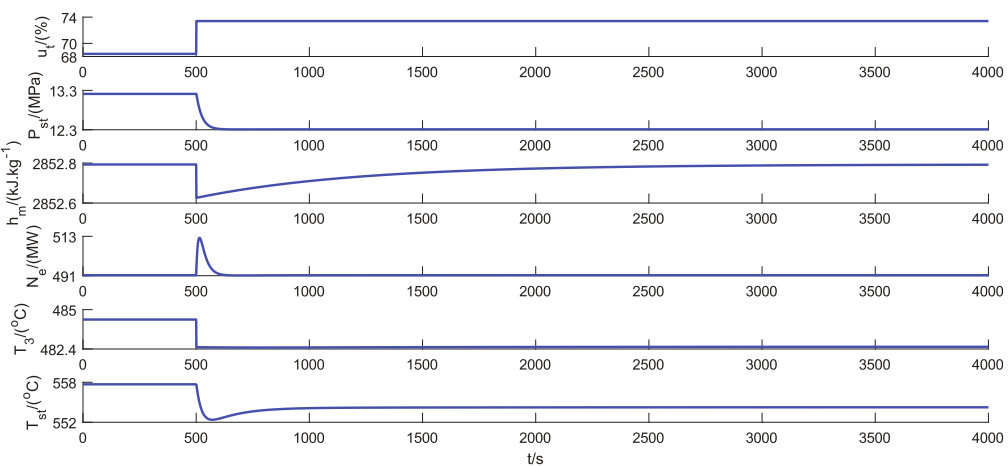


Fig. 8. Step responses of the OTBT model to throttle valve opening.

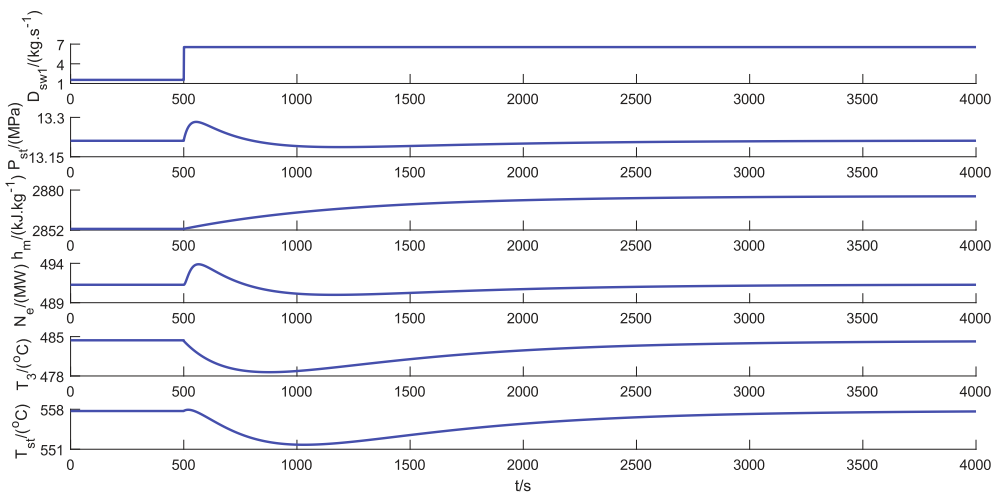


Fig. 9. Step responses of the OTBT model to primary spray water flow.

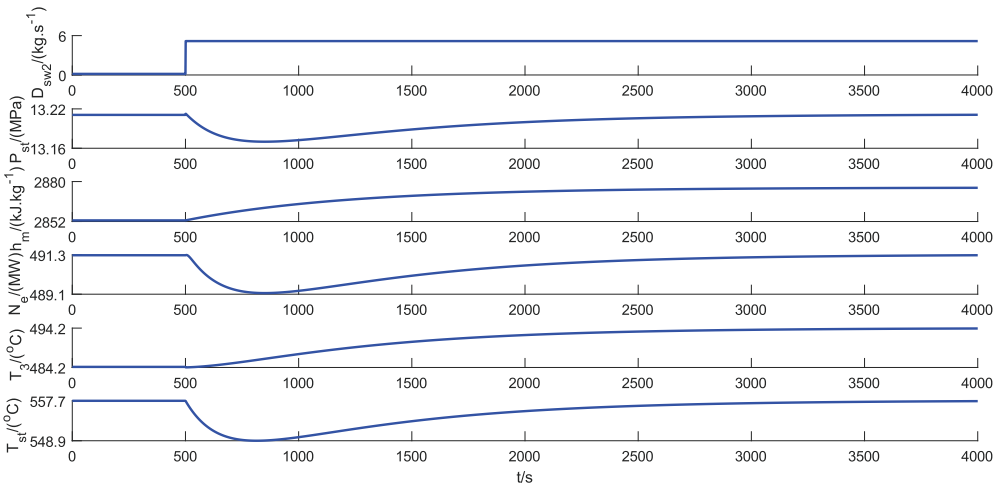


Fig. 10. Step responses of the OTBT model to secondary spray water flow.

2852.8 kJ/kg to 2852.6 kJ/kg quickly, and gradually restores to the original value on account of unchanged ratio of coal to water. Similarly, with more steam pushing into turbine, unit load promptly increases from 491.3 MW to 512.2 MW, and then gradually decreases to the original value after releasing heat energy stored in boiler.

Fig. 9 shows responses to a step increase of primary spray water. When primary spray water flow raises abruptly by 5 kg/s, steam in superheaters gets squeezed, and output variables start to change after time delay of 2s. As the steam is squeezed and primary spray water absorbs heat energy in superheaters, main steam pressure,  $P_{st}$ , increases quickly from 13.21 MPa to 13.28 MPa, and gradually restores to 13.21 MPa after the squeezing effect. Accordingly, feedwater entering into economizer, and thus steam enthalpy in separator,  $h_m$ , gradually increases from 2852.8 kJ/kg to 2875.6 kJ/kg, where its time constant is 716s. As more steam enters into turbines, unit load quickly raises from 491.3 MW to 493.9 MW, and gradually decreases to the original value due to unchanged feedwater and coal flows. For steam temperature, the purpose of primary spray water is to control the temperature of steam at the output of platen superheater, and thus  $T_3$  gradually declines from 484.3 °C to 478.7 °C, and then slowly increases to 484.1 °C. Similarly, due to the squeezing effect,  $T_{st}$  raises abruptly from 557.7 °C to 557.9 °C. When steam with relatively low temperature enters into the superheater,  $T_{st}$  gradually decreases from 557.9 °C to 551.8 °C, and slowly restores to 557.6 °C due to unchanged total feedwater flow.

Fig. 10 shows responses to a step increase of secondary spray water. When the secondary spray water flow raises abruptly by 5 kg/s, steam

in superheaters is squeezed slightly, and output variables start to change after time delay of 2s. With steam temperature decreasing in high temperature superheater,  $P_{st}$  gradually decreases from 13.21 MPa to 13.17 MPa, and lastly restores to 13.21 MPa due to unchanged total feedwater flow. Similarly, unit load,  $N_e$ , and  $T_{st}$  gradually decreases from 491.3 MW and 557.7 °C to 489.2 MW and 548.9 °C, respectively, due to increased secondary spray water. As total feedwater flow keeps unchanged,  $N_e$  and  $T_{st}$  gradually restore to 491.3 MW and 557.6 °C, respectively. As feedwater entering into economizer decreases,  $T_3$  and  $h_m$  gradually increase from 484.3 °C and 2852.8 kJ/kg to 494.1 °C and 2875.6 kJ/kg, respectively, due to unchanged coal flow, where their time constants are 958s and 716s, respectively.

From the responses in Figs. 6–10 and their analysis, dynamic behaviors of our model are in accordance with operational experience, which illustrates that model established can be used for simulation analysis.

## 6. Conclusion

In this paper, a dynamic nonlinear model for superheated steam temperature and coordinated control systems of once-through boiler units is developed. The model structure is derived from mass and energy conservation laws, and the control structure based on the model is presented and analyzed. Parameters and functions in the model are identified based on operational data by using nonlinear regression analysis and immune genetic algorithm. Lastly, open-loop simulation

and dynamic validation were conducted to prove satisfactory performances of the model established. Based on the above analysis and work, conclusions are drawn as follows:

- (1) The model reflects that spray water can influence the stability of intermediate-point enthalpy, which accords with practical operation.
- (2) The model presents that spray water adjusts superheated steam temperature quickly, and total feedwater flow determine the final value of superheated steam temperature at steady-state conditions, which complies with the control concept of superheated steam temperature for once-through boiler-turbine units.
- (3) The model structure can reflect the varying inertia time and nonlinear characteristics of superheated steam temperature system under different loading conditions.
- (4) This work presents a method of improving model accuracy, and

## Appendix A

### A.1. Case A

- (1). Operational time is from 101s to 5814s:

$$\begin{aligned}\theta_3 &= \{-5.33, -3.4, 1.56, 184\}, \\ \theta_4 &= \{-4.36, 4.71, 0.77, 452\}, \\ \theta_5 &= \{-37.32, -2.84, 2.45, 471\}.\end{aligned}$$

- (2). Operational time is from 5815s to 30514s:

$$\begin{aligned}\theta_3 &= \{-48.29, 3.79, 1.46, 498\}, \\ \theta_4 &= \{48.49, 4.36, -0.49, 415\}, \\ \theta_5 &= \{-49.95, -3.17, 2.48, 325\}.\end{aligned}$$

- (3). Operational time is from 30515s to 53740s:

$$\begin{aligned}\theta_3 &= \{-18.1, 2.29, 0.99, 344\}, \\ \theta_4 &= \{-46.6, -4.23, 3.26, 257\}, \\ \theta_5 &= \{9.59, -2.25, 0.88, 254\}.\end{aligned}$$

- (4). Operational time is from 53741s to 84892s:

$$\begin{aligned}\theta_3 &= \{-19.08, 0.29, 1.32, 453\}, \\ \theta_4 &= \{-49.94, 4.31, 1.89, 14\}, \\ \theta_5 &= \{-49.57, -3.45, 2.32, 346\}.\end{aligned}$$

- (5). Operational time is from 84893s to 102080s:

$$\begin{aligned}\theta_3 &= \{23.51, 2.1, 0.2, 493\}, \\ \theta_4 &= \{-49.9, -4.86, 3.4, 24\}, \\ \theta_5 &= \{2.92, 2.78, 0.22, 470\}.\end{aligned}$$

### A.2. Case B

- (1). Operational time is from 101s to 21498s:

$$\begin{aligned}\theta_3 &= \{5.53, -9.61, 2.25, 21\}, \\ \theta_4 &= \{46.49, 4.62, -0.58, 148\}, \\ \theta_5 &= \{21.69, 3.93, 0.05, 375\}.\end{aligned}$$

correction factors of heat functions are modeled. Results reflect that model accuracy can be improved at least 50% by comparison.

- (5) Open-loop responses of the model developed are in accordance with operational experience, and the model has a proper physical structure with a general and simple form. It indicates that the model can be used for simulation analysis and controller design.

In future, advanced control algorithms will be designed and tested based on this model in order to further improve control performance of superheated steam temperature system and coordinated control system.

## Declaration of Competing Interest

The authors declare that they have no known competing financial interests or personal relationships that could have appeared to influence the work reported in this paper.

(2). Operational time is from 21499s to 63970s:

$$\begin{aligned}\theta_3 &= \{-3, -0.95, 1.17, 78\}, \\ \theta_4 &= \{-28.95, -2.13, 1.99, 437\}, \\ \theta_5 &= \{0.46, 4.55, 0.38, 190\}.\end{aligned}$$

(3). Operational time is from 63971s to 95369s:

$$\begin{aligned}\theta_3 &= \{-4.3, -1.68, 1.31, 93\}, \\ \theta_4 &= \{-4.02, 2.14, 1.05, 494\}, \\ \theta_5 &= \{-16.49, -1.71, 1.44, 479\}.\end{aligned}$$

(4). Operational time is from 95370s to 105046s:

$$\begin{aligned}\theta_3 &= \{6.39, -4.6, 1.52, 82\}, \\ \theta_4 &= \{-46.86, 0.65, 1.94, 204\}, \\ \theta_5 &= \{-40.25, 4.62, 1.02, 145\}.\end{aligned}$$

(5). Operational time is from 105047s to 121890s:

$$\begin{aligned}\theta_3 &= \{0.83, -3.31, 1.42, 313\}, \\ \theta_4 &= \{-14.87, 1.42, 1.16, 383\}, \\ \theta_5 &= \{-29.16, -0.58, 1.63, 133\}.\end{aligned}$$

## Appendix B. Supplementary material

Supplementary data associated with this article can be found, in the online version, at <https://doi.org/10.1016/j.aplthermaleng.2020.114912>.

## References

- [1] D. Zhang, J. Wang, Y. Lin, Present situation and future prospect of renewable energy in China, *Renew. Sustain. Energy Rev.* 76 (2017) 865–871.
- [2] H. Dai, X. Xie, Y. Xie, Green growth: the economic impacts of large-scale renewable energy development in China, *Appl. Energy* 162 (2016) 435–449.
- [3] A.L. D'Agostino, B.K. Sovacool, M.J. Bambawale, And then what happened? A retrospective appraisal of china's renewable energy development project (redp), *Renew. Energy* 36 (11) (2011) 3154–3165.
- [4] Falah AlObaid, Nicolas Mertens, Ralf Starkloff, Thomas Lanz, Christian Heinze, Bernd Epple, Progress in dynamic simulation of thermal power plants, *Prog. Energy Combust. Sci.* 59 (2017) 79–162.
- [5] Deliang Zeng, Yaokui Gao, Hu. Yong, Jizhen Liu, Optimization control for the coordinated system of an ultra-supercritical unit based on stair-like predictive control algorithm, *Control Eng. Pract.* 82 (2019) 185–200.
- [6] L. Sun, Q. Hua, J. Shen, Y. Xue, D. Li, K.Y. Lee, Multi-objective optimization for advanced superheater steam temperature control in a 300 MW power plant, *Appl. Energy* 208 (2017) 592–606.
- [7] Z. Wu, T. He, D. Li, Y. Xue, L. Sun, L. Sun, Superheated steam temperature control based on modified active disturbance rejection control, *Control Eng. Pract.* 83 (2019) 83–97.
- [8] K.J. Åström, R. Bell, Dynamic models for boiler-turbine alternator units: Data logs and parameter estimation for a 160 MW unit. Technical report, 1987.
- [9] F.P. De Mello, Boiler models for system dynamic performance studies, *IEEE Trans. Power Syst.* 6 (1) (1991) 66–74.
- [10] G. Hou, H. Du, Y. Yang, Coordinated control system modelling of ultra-supercritical unit based on a new TS fuzzy structure, *ISA Trans.* 74 (2018) 120–133.
- [11] D. Strušnik, M. Golob, J. Avsec, Artificial neural networking model for the prediction of high efficiency boiler steam generation and distribution, *Simul. Model. Pract. Theory* 57 (2015) 58–70.
- [12] Jonghoon Ahn, Soolyeon Cho, Dae Hun Chung, Analysis of energy and control efficiencies of fuzzy logic and artificial neural network technologies in the heating energy supply system responding to the changes of user demands, *Appl. Energy* 190 (2017) 222–231.
- [13] Kornel Rostek, Łukasz Morytko, Anna Jankowska, Early detection and prediction of leaks in fluidized-bed boilers using artificial neural networks, *Energy* 89 (2015) 914–923.
- [14] Guolian Hou, Linjuan Gong, Congzhi Huang, Jianhua Zhang, Novel fuzzy modeling and energy-saving predictive control of coordinated control system in 1000 MW ultra-supercritical unit, *ISA Trans.* 86 (2019) 48–61.
- [15] Henrique Pomeiro, Rodolfo Santos, Paulo Carreira, Carlos Silva, Joao M.C. Sousa, Comparative assessment of low-complexity models to predict electricity consumption in an institutional building: linear regression vs. fuzzy modeling vs. neural networks, *Energy Build.* 146 (2017) 141–151.
- [16] J.Z. Liu, S. Yan, D.L. Zeng, A dynamic model used for controller design of a coal fired once-through boiler-turbine unit, *Energy* 93 (2015) 2069–2078.
- [17] H. Fan, Y. Zhang, Z. Su, A dynamic mathematical model of an ultra-supercritical coal fired once-through boiler-turbine unit, *Appl. Energy* 189 (2017) 654–666.
- [18] D. Wang, Y. Zhou, H. Zhou, A mathematical model suitable for simulation of fast cut back of coal-fired boiler-turbine plant, *Appl. Therm. Eng.* 108 (2016) 546–554.
- [19] Wiesław Zima, Simulation of rapid increase in the steam mass flow rate at a supercritical power boiler outlet, *Energy* 173 (2019) 995–1005.
- [20] Y. Zhou, D. Wang, An improved coordinated control technology for coal-fired boiler-turbine plant based on flexible steam extraction system, *Appl. Therm. Eng.* 125 (2017) 1047–1060.
- [21] C. Sreepradha, R.C. Panda, N.S. Bhuvaneswari, Mathematical model for integrated coal fired thermal boiler using physical laws, *Energy* 118 (2017) 985–998.
- [22] L. Sun, D. Li, K.Y. Lee, Control-oriented modeling and analysis of direct balance in coal-fired boiler-turbine unit, *Control Eng. Pract.* 55 (2016) 38–55.
- [23] Chandrasekharan Sreepradha, Rames Chandra Panda, Natrajan Swaminathan Bhuvaneswari, Mathematical model for integrated coal fired thermal boiler using physical laws, *Energy* 118 (2017) 985–998.
- [24] Hamed Hajebzadeh, Adulhamid N.M. Ansari, Saeid Niazi, Mathematical modeling and validation of a 320 MW tangentially fired boiler: a case study, *Appl. Therm. Eng.* 146 (2018) 232–242.
- [25] Z. Hong, C. Cheng, J. Lai, X. Lu, Q. Deng, X. Gao, Z. Lei, Affine nonlinear control for an ultra-supercritical coal fired once-through boiler-turbine unit, *Energy* 153 (2018) 638–649.
- [26] M. Lawryńczuk, Nonlinear predictive control of a boiler-turbine unit: a state-space approach with successive on-line model linearisation and quadratic optimisation, *ISA Trans.* 67 (Complete) (2017) 476–495.
- [27] Martin Klaučo, Michal Kvasnica, Control of a boiler-turbine unit using mpc-based reference governors, *Appl. Therm. Eng.* 110 (2017) 1437–1447.
- [28] Y. Zhao, C. Wang, M. Liu, D. Chong, J. Yan, Improving operational flexibility by regulating extraction steam of high-pressure heaters on a 660MW supercritical coal-fired power plant: a dynamic simulation, *Appl. Energy* 212 (2018) 1295–1309.
- [29] R. Starkloff, F. AlObaid, K. Karner, B. Epple, M. Schmitz, F. Boehm, Development

- and validation of a dynamic simulation model for a large coal-fired power plant, *Appl. Therm. Eng.* 91 (2015) 496–506.
- [30] K.J. Åström, R.D. Bell, Drum-boiler Dynamics, *Automatica* 36 (3) (2000) 363–378.
- [31] J. Adams, D.R. Clark, J.R. Louis, J.P. Spanbauer, Mathematical modeling of once-through boiler dynamics, *IEEE Trans. Power App. Syst.* 84 (2) (1965) 146–156.
- [32] Yuguang Niu, Ming Du, Weichun Ge, Huanhuan Luo, Guiping Zhou, A dynamic nonlinear model for a once-through boiler-turbine unit in low load, *Appl. Therm. Eng.* (2019) 113880.
- [33] Zhang Fan, Wu Xiao, and Jiong Shen, Jiong Shen, Extended state observer based fuzzy model predictive control for ultra-supercritical boiler-turbine unit, *Appl. Therm. Eng.* 118 (Complete) (2017) 90–100.
- [34] Lu. Hong-bo, Yu. Zhang, Wu. Chang-kai, Wei-hua Sun, Dynamic model identification of the main steam temperature for supercritical once-through boiler, *Energy Procedia* 17 (2012) 1704–1709.
- [35] Nahla Alamoodi, Prodromos Daoutidis, Nonlinear control of coal-fired steam power plants, *Control Eng. Pract.* 60 (2017) 63–75.
- [36] Tian Haijun, Wang Jingru, Modeling of power plant superheated steam temperature based on least squares support vector machines, *Energy Procedia* 17 (2012) 61–67.
- [37] Wen-Jie Zhao, Yug-Uang Niu, Ji-Zhen Liu, Multi-model adaptive control for the superheated steam temperature, *Proceedings. International Conference on Machine Learning and Cybernetics*, vol. 1, IEEE, 2002, pp. 269–272.
- [38] A. Leva, C. Maffezzoni, G. Benelli, Validation of drum boiler models through complete dynamic tests, *Control Eng. Pract.* 7 (1) (1999) 11–26.